

J. Garcia, J.F. Artaud, V. Basiuk, M. Brix, J. Decker, G. Giruzzi, N. Hawkes,
F. Imbeaux, X. Litaudon, J. Mailloux, Y. Peysson, M. Schneider
and JET EFDA contributors

RF-Driven Advanced Modes of ITER Operation

“This document is intended for publication in the open literature. It is made available on the understanding that it may not be further circulated and extracts or references may not be published prior to publication of the original when applicable, or without the consent of the Publications Officer, EFDA, Culham Science Centre, Abingdon, Oxon, OX14 3DB, UK.”

“Enquiries about Copyright and reproduction should be addressed to the Publications Officer, EFDA, Culham Science Centre, Abingdon, Oxon, OX14 3DB, UK.”

The contents of this preprint and all other JET EFDA Preprints and Conference Papers are available to view online free at www.iop.org/Jet. This site has full search facilities and e-mail alert options. The diagrams contained within the PDFs on this site are hyperlinked from the year 1996 onwards.

RF-Driven Advanced Modes of ITER Operation

J. Garcia¹, J.F. Artaud¹, V. Basiuk¹, M. Brix², J. Decker¹, G. Giruzzi¹, N. Hawkes²,
F. Imbeaux¹, X. Litaudon¹, J. Mailloux², Y. Peysson¹, M. Schneider¹
and JET EFDA contributors*

JET-EFDA, Culham Science Centre, OX14 3DB, Abingdon, UK

¹*CEA, IRFM, F-13108 Saint-Paul-lez-Durance, France.*

²*EURATOM-UKAEA Fusion Association, Culham Science Centre, OX14 3DB, Abingdon, OXON, UK*

** See annex of F. Romanelli et al, "Overview of JET Results",
(Proc. 22nd IAEA Fusion Energy Conference, Geneva, Switzerland (2008)).*

Preprint of Paper to be submitted for publication in Proceedings of the
18th Topical Conference on Radio Frequency Power in Plasmas, Gent, Belgium.
(22nd June 2009 - 24th June 2009)

ABSTRACT.

The impact of the Radio Frequency heating and current drive systems on the ITER advanced scenarios is analyzed by means of the CRONOS suite of codes for integrated tokamak modelling. As a first step, the code is applied to analyze a high power advanced scenario discharge of JET in order to validate both the heating and current drive modules and the overall simulation procedure. Then, ITER advanced scenarios, based on Radio Frequency systems, are studied on the basis of previous results. These simulations show that both hybrid and steady-state scenarios could be possible within the ITER specifications, using RF heating and current drive only.

1. INTRODUCTION

The advanced scenarios in ITER, i.e. the so called hybrid and steady-state scenarios, rely on the capability for controlling both the heating channel and the current density profile. In the case of the steady-state, the power source that sustains the burn must be partly generated by the plasma itself, via self-heating due to the energetic alpha particles produced by the fusion reactions. In addition, a large fraction of the current flowing in the plasma and necessary for the stability of the magnetic configuration should also be self-generated by the bootstrap effect, which could be obtained in the presence of an Internal Transport Barrier (ITB) [1]. This implies that a localised control of heating, current drive and bootstrap current is necessary to sustain ITBs for a long time. However, this is notoriously difficult when the bootstrap fraction is the dominant contribution (current alignment problem). For hybrid scenarios, the zero loop voltage constraint is removed and, although no ITB is foreseen, the control of the q profile is still an issue, since q above 1 is required in this regime. In this framework, the Radio Frequency (RF) heating systems can provide a conceptual solution to this problem since the power and Current Drive (CD) deposition can be well localized, leading to controlled q profiles.

In this paper the integrated tokamak modelling suite of codes CRONOS [2] is applied to analyze the importance of the RF systems to establish stable steady-state and hybrid scenarios in two different machines, JET and ITER. As a first step, a high power advanced scenario discharge of JET will be analyzed, and used for validation of the various modules entering the CRONOS suite. The impact of adding an extra source of off-axis CD, e.g., Electron Cyclotron Resonant Heating and Current Drive (ECRH/ECCD) to improve the performances of such advanced scenarios on JET will be investigated. For ITER, different heating mixes will be considered, for both hybrid and steady-state scenarios.

2. THE CRONOS CODE

These studies have been performed by means of the CRONOS suite of codes, which solves the transport equations for various plasma fluid quantities (current, energy, matter, momentum). This is done in one dimension (the magnetic flux coordinate associated with the minor radius), self-consistently with 2-dimensional magnetic equilibrium. In particular, the fusion power is evaluated

here by the orbit following Monte-Carlo code SPOT [3], which is of special interest here, since reversed q profiles can be obtained, which could have an impact on the alpha particle confinement. The Lower Hybrid Current Drive (LHCD) power deposition and driven current have been computed inside CRONOS by means of the LUKE/C3PO code [4], i.e., a 3D Fokker-Planck code coupled to toroidal ray-tracing. The Neutral Beam Current Drive (NBCD) is calculated by means of the Monte-Carlo code NEMO/SPOT. The ECRH/ECCD is calculated by means of REMA [5] (ray-tracing and relativistic damping of electron cyclotron waves), with a linear estimate of the ECCD efficiency [6]. Finally, the Ion Cyclotron Resonant Heating (ICRH) is calculated with PION [7]. Fully time dependent simulations are performed, both interpretative and predictive for JET discharges, which is useful in order to select the most appropriate transport model available in CRONOS [2]. For ITER, predictive simulations lasting as long as 3000s are performed.

4. ANALYSYS OF THE JET ADVANCED PULSE NO: 77895

As a first step to analyze the importance of the RF systems for the advanced scenarios in ITER, a specific evaluation of the CRONOS capability to simulate such scenarios in JET real experiments has been done. In particular the shot 77895 has been analyzed by both interpretative and predictive simulations. The main characteristics of this shot are: a total current $I_p=1.75\text{MA}$, toroidal magnetic field $B_t=2.7\text{T}$ and $q_{95}=5$. For this shot 23MW of NBI, 7MW of ICRH and 2 MW of LH (with $n_{||}=1.84$) were used. With this configuration, an average $\beta_N=2.7$ has been obtained. First, an interpretative simulation of the shot has been done by using the experimental data available (density and temperature profiles, equilibrium data) and simulating the evolution of the current density profiles. In figure 1, the experimental temperatures and electron density (obtained with High Resolution Thomson Scattering (HRTS) and Charge-Exchange spectroscopy (CXFM)) as well as the calculated current density profiles and time dependent q profile evolution are shown. The current density profile is determined by the NBCD in the plasma center, the LH at $\rho=0.6$ and by the bootstrap current. Therefore, the total non-inductive current obtained is 1.2MA (with $I_{nbi}=0.35\text{MA}$, $I_{lh}=0.23\text{MA}$ and $I_{boot}=0.65\text{MA}$) which represents $f_{ni}=69\%$ and $f_{boot}=35\%$. The internal inductance obtained with this configuration is $l_i=0.72$, which is quite close to the experimental value, 0.70.

Regarding the time evolution of the q profile, the profiles obtained with CRONOS are in agreement with experimental data as shown in figure 2. At the beginning of the flap top phase, $t=5\text{s}$, it is slightly above 2, however, due to the current penetration, it slowly drops, being close to $q=1$ at the end of this phase. Therefore, according to these calculations, this scenario is not well sustained due to the current penetration, misalignment of the currents and lack of enough bootstrap current.

With the aim of analyzing the temperatures that could be obtained by changing the heating mix, a predictive simulation of the temperatures and currents evolution has been carried out with the Bohm-GyroBohm [8] model which was formerly determined from the analysis of a large number of JET discharges. Since an ITB is present in the ion channel, the experimental rotation has been

used to calculate the anomalous transport suppression according to the expression used in [9]. In figure 3, the simulated ion and electron temperatures are compared to the experimental data. Although the pedestal height for both channels is not completely well simulated, with a difference of $\approx 15\%$, the global shape of the profiles is good, leading to a difference in the total bootstrap current of only 5%. The strength of the ion ITB is underestimated, since the gradient obtained is lower, however this fact only leads to a difference in the central temperature of 0.8 keV. Therefore, this model gives reasonable results for the temperature profiles and can be used to analyze the impact of adding an extra source of off-axis CD, in order to control the current alignment and increase the bootstrap fraction.

10MW of ECRH/ECCD power are added at $\rho = 0.5$ with the aim of solving the problems of stability of the q profile by having more non-inductive current. The results obtained at the end of the flat-top phase are shown in figure 4. The ion temperature sharply increases up to 12keV and a weak ITB is also formed in the electron channel, for which the central temperature reaches 9.5keV. The reason for this behavior is that the ECCD deposition is well localised at $\rho = 0.5$ with a very peaked profile, which leads to a region of negative magnetic shear and the suppression of turbulent transport (according to the physics ingredient of the BohmgyroBohm model). The deposition of the other current drive sources do not change significantly, with the LH deposition remaining at $\rho = 0.65$. The fact that stronger ITB are obtained with this current scheme leads to a much higher bootstrap current fraction of $f_{\text{boot}} = 45\%$ which together with the ECCD current, $I_{\text{eccd}} = 0.24\text{MA}$, increases the total non-inductive current fraction up to $f_{\text{ni}} = 85\%$. In this case, the q profile does not drop so fast as in the original shot, due to the fact that more non-inductive current is in the plasma and that a new region with negative magnetic shear appears. However, the q profile can not be sustained above 2, and still a region with positive shear appears at $\rho < 0.5$. In that region, the q profile is mainly determined by the large amount of current driven by the NBI system, and in addition, the new bootstrap current generated is also located in $\rho < 0.5$. In the next section, it will be shown that this is a fundamental problem for the steady-state sustainment of ITB's.

5. ITER STEADY-STATE RF-SCENARIO

In order to study the ITB formation for ITER in reversed shear scenarios, a model for the reduction of turbulent transport in such regimes is needed. Since no model is able to simulate ITB time dependent formation and sustainment for all the present day tokamaks [10], the heat diffusivity model of the type used in reference [11] is adopted, i.e., $\chi_i = \chi_e = \chi_{i,\text{neo}} + 0.4(1+3\rho^2)F(s)$, F is a shear function (vanishing for $s < 0$). This model has been extensively used to establish the ITER reference scenarios with ITB [12] and it is based on the experimental results obtained in JT-60U [13] with ITB shots. It must be considered as a kind of minimal model which is used here to ensure that the phenomena here analyzed do not depend on specific ingredients of models, but only on their common feature: the confinement improvement associated with $s < 0$. Since the pedestal main features cannot be predicted with enough accuracy, the pedestal temperature is fixed at $\rho \approx 0.93$ $T_{\text{ped}} \approx 3\text{keV}$, which is a conservative value with respect to the different scaling available for this

parameter in the ITER H mode [14]. The electron density profile is prescribed with a ramp in the early phase of the regime, then fixed to a Greenwald limit fraction of $f_G = 0.9$, and the global parameters for the ITER steady-state reference scenario 4 have been considered [6], except the total current, which has been downscaled to 8MA.

In order to avoid shrinking or erosion of the ITB, a method is needed to control the dominant current component, i.e., the bootstrap current, which is in turn essentially related to the dominant heating source, i.e., the alpha heating. As previously seen for JET, the fact that the current drive from the NBI system is naturally located (even for ITER) inside the expected location of the ITB makes the control of this current difficult. Therefore, in this paper a pure RF scenario without NBI has been considered, which is obtained using $P_{IC} \approx 20\text{MW}$, $P_{EC} \approx 20\text{MW}$, $P_{LH} \approx 13\text{MW}$. With the aim of maximizing the alpha power obtained at the minimum input power, the 20 MW of EC power are deposited at $r \approx 0.5$ by using 12MW from the Upper Steering Mirrors of the Top Launcher at $\phi_{\text{tor}} = 20^\circ$ (fixed) and $\phi_{\text{pol}} = 67^\circ$ and 8MW from Upper Row of the Equatorial Launcher at $\phi_{\text{tor}} = 38^\circ$ and $\phi_{\text{pol}} = 0^\circ$ (fixed) [15].

The time evolution of H_{98} , bootstrap current fraction, Greenwald fraction, and total non-inductive current fraction are shown in figure 5 (a). The bootstrap current fraction (=77%) is stable during all the simulation and represents the main contribution to the total non-inductive current fraction. The plasma is above the estimated no-wall stability limit ($\beta_N > 4I_i$), owing to the flatness of the current density profile. The H_{98} factor (=1.7) obtained is high, however, it is worth to point out that, since no NBI system is used, higher levels of bootstrap current fraction (and therefore higher H_{98}) are expected because the current drive efficiency of the RF systems is smaller. Nevertheless, the inclusion of a NBI system leads to stability problems of the same kind as previously reported for JET, the q profile drops in the central region and the negative magnetic shear region is lost after some current diffusion times. This is due to the minimum magnetic shear needed to sustain this scenario [16]. Therefore, in order to overcome this problem, an off-axis NBI heating system would be preferred in ITER.

The time evolution of the input, alpha and radiated power is shown in figure 5(b). The alpha power obtained fluctuates in time since a Monte-Carlo code has been used to calculate it, however its average is stable with a value of 70MW which allows a fusion gain of $Q = 6.5$. The radiated power is $P_{\text{rad}} = 40\text{MW}$, with a high contribution by both synchrotron, 10MW, and bremsstrahlung radiation, 15MW. The plasma density, the electron and ion temperature profiles as well as the current density profiles obtained at $t = 3000\text{s}$ and the evolution of the q profile from $t = 2000\text{s}$ are shown in figure 6. The current density profile obtained shows a maximum at $\rho = 0.45$, which is at the maximum both of, the bootstrap current and of the ECCD. Therefore, the ECCD locks the ITB at mid-radius and avoids its erosion and shrinking [17]. The LH power deposition is located at $\rho = 0.7$, and the current drive obtained ($\approx 0.6\text{MA}$) contributes to the total non-inductive current fraction ($\phi_{\text{ni}} \approx 97\%$). A small amount of central current drive (e.g., by fast waves, $I_{\text{fwcd}} = 20\text{kA}$) is added in order to control q_0 . This current prevents excessive increase of q_0 , which would imply loss of alpha

particle confinement [3]. With this current drive scheme, the q profile obtained is stable for 1000s, as shown in figure 6, with $q_0 \approx 6$ and $q_{\min} > 2$. With the transport model used, the reversed q allows a reduction of anomalous transport close to the ion neoclassical level, which finally leads to a temperature profile rather flat in the plasma core, and a large normalized temperature gradient, $R/L_{te} = 27$ (where R is the plasma major radius with T_e the electron temperature), at $\rho = 0.45$ as shown in figure 6.

It is worth to point out that the heating and current combination used for this scenario is quite similar to the JET Advanced Tokamak scenario where ECRH/ECCD has been added as studied in the previous section. The only difference comes from the fact that in this case, the NBI power has been removed to avoid the drop of the central q profile region due to the NBCD. This fact can be possible because the central heating necessary for JET is obtained in ITER by means of the alpha power.

Following the general guidelines and parameters for the ITER hybrid scenario proposed in ref. [18]. One of the main characteristics of this scenario is to have a q profile above 1, which avoids sawteeth. The impact of the heating mix has been analyzed and in particular the 33MW of NBI power have been replaced by the same amount of ECRH/ECCD power. In addition, the pedestal height has been dropped, in comparison with ref. [16], to 4keV, with the aim of avoiding optimistic bootstrap current from the edge. The transport model used here is GLF23 [19]. In figure 7, a comparison between the temperatures, current density profiles and evolution of the q profile is shown. The central electron temperature increases by 1keV when the ECRH/ECCD heating is used, whereas the ion temperature slightly drops, due to the decrease of ion heating. Therefore the fusion gain drops from $Q = 5.5$ in the NBI case to 5. Regarding the current density profiles, the off-axis NBCD deposition, $I_{nbi} = 2.2\text{MA}$, is rather broad. On the other hand, the ECCD deposition, $I_{eccd} = 1.0\text{MA}$, is well localized at $\rho = 0.35$. This difference has a significant effect on the current density profile, creating a local maximum at the same radial position where the ECCD is located. The evolution of the q profile is affected by this fact since, although the time to have $q_0 = 1$ is the same for both heating schemes the extension of the $q_0 < 1$ region is reduced from $0 < \rho < 0.37$ to $0 < \rho < 0.2$. This shows that an accurate control of the current density profiles may be essential for the ITER hybrid scenario. For that purpose, LH will be also considered in the future.

CONCLUSIONS

The impact of the RF-systems on JET and ITER advanced scenarios has been analyzed in this paper. As a first step to understand the different capabilities of the present day heating and current drive systems, the JET advanced Pulse No: 77895 has been analyzed and simulated with the CRONOS suite of codes.

According to the calculations performed for the Pulse No: 77895 the current density profile is mainly determined by the different external non-inductive current drive capability and the bootstrap current. In particular, the NBCD highly determines the central plasma and the LH and bootstrap current at the edge. It has been shown that the addition of 10MW of ECRH/ECCD with the same

plasma conditions can lead to a plasma close to $V_{loop} = 0$ with a more stable q profile. However, there are still difficulties to have steady reversed magnetic shear plasmas due to the strong effect of the NBCD in the central zone.

The same effects are found when trying to establish a steady state scenario in ITER simulations. In order to solve these problems, a new scenario for ITER steady-state plasmas with only RF heating systems is proposed by means of the creation and sustainment of ITB for 3000s. This scenario provides a solution to the current alignment problem, which caused the shrinking and erosion of the ITB in previous studies performed with NBI current drive. The main feature of this scenario is that there is a minimum negative magnetic shear required in order to steadily sustain the ITB for 3000s [16]. The present design of the EC power system in ITER can provide such a negative magnetic shear at $\rho = 0.45$ through ECCD, which finally locks the ITB and avoids the current penetration. In addition, the LH power helps to sustain this scenario by providing current outside the ITB.

Finally, the RF-systems provide a good control means for the ITER hybrid scenario. Although the fusion gain slightly drops compare to that obtained with a NBI system, the control of q_0 becomes easier and the region with $q_0 < 1$ is reduced.

ACKNOWLEDGMENTS

This work, supported by the European Communities under the contract of Association between EURATOM and CEA, was carried out within the framework of the European Fusion Development Agreement. The views and opinions expressed herein do not necessarily reflect those of the European Commission

REFERENCES

- [1]. X. Litaudon, Plasma Phys. Control. Fusion **48**, A1 (2006).
- [2]. V. Basiuk et al., Nucl. Fusion **43**, 822 (2003).
- [3]. M. Schneider et al., Plasma Phys. Control. Fusion **47**, 2087 (2005).
- [4]. Y. Peysson and J. Decker 2007 EPS Conf. on Plasma Phys. (Warsaw) vol **31F** (ECA) P-4.164.
- [5]. V. Krivenski et al., Nucl. Fusion **25** 127 (1985).
- [6]. Y.R. Lin-Liu, V.S. Chan and R. Prater, Phys. Plasmas **10** 4064 (2003).
- [7]. L.-G. Eriksson et al, Nucl. Fusion **33**, 1037 (1993).
- [8]. M.Erba et al., Plasma Phys. Control. Fusion **39**, 261 (1997).
- [9]. T. Tala et al., Plasma Phys. Control. Fusion **43**, 507 (2001).
- [10]. T. Tala et al., Nucl. Fusion **46**, 548 (2006).
- [11]. A.R. Polevoi et al., 19th IAEA Fusion Energy Conf. (Lyon, 2002) file CT/P-08.
- [12]. C. Gormezano et al., Nucl. Fusion **47** S285–S336 (2007).
- [13]. T. Fujita et al., Phys. Rev. Lett. **78**, 2377 (1997).
- [14]. M. Sugihara et al., Plasma Phys. Controlled Fusion **45**, L55 (2003).

- [15]. G. Ramponi et al., Fus. Sci. Techn. **52**, 193 (2007).
 [16]. J. Garcia et al., Phys. Rev. Lett. **100**, 255004 (2008).
 [17]. M. Murakami et al., Phys. Rev. Lett. **90**, 255001 (2003).
 [18]. C. Kessel et al., Nucl. Fus. **47** 1274–1284 (2007).
 [19]. J.E. Kinsey et al., Phys. Plasmas **12** 052503 (2005).

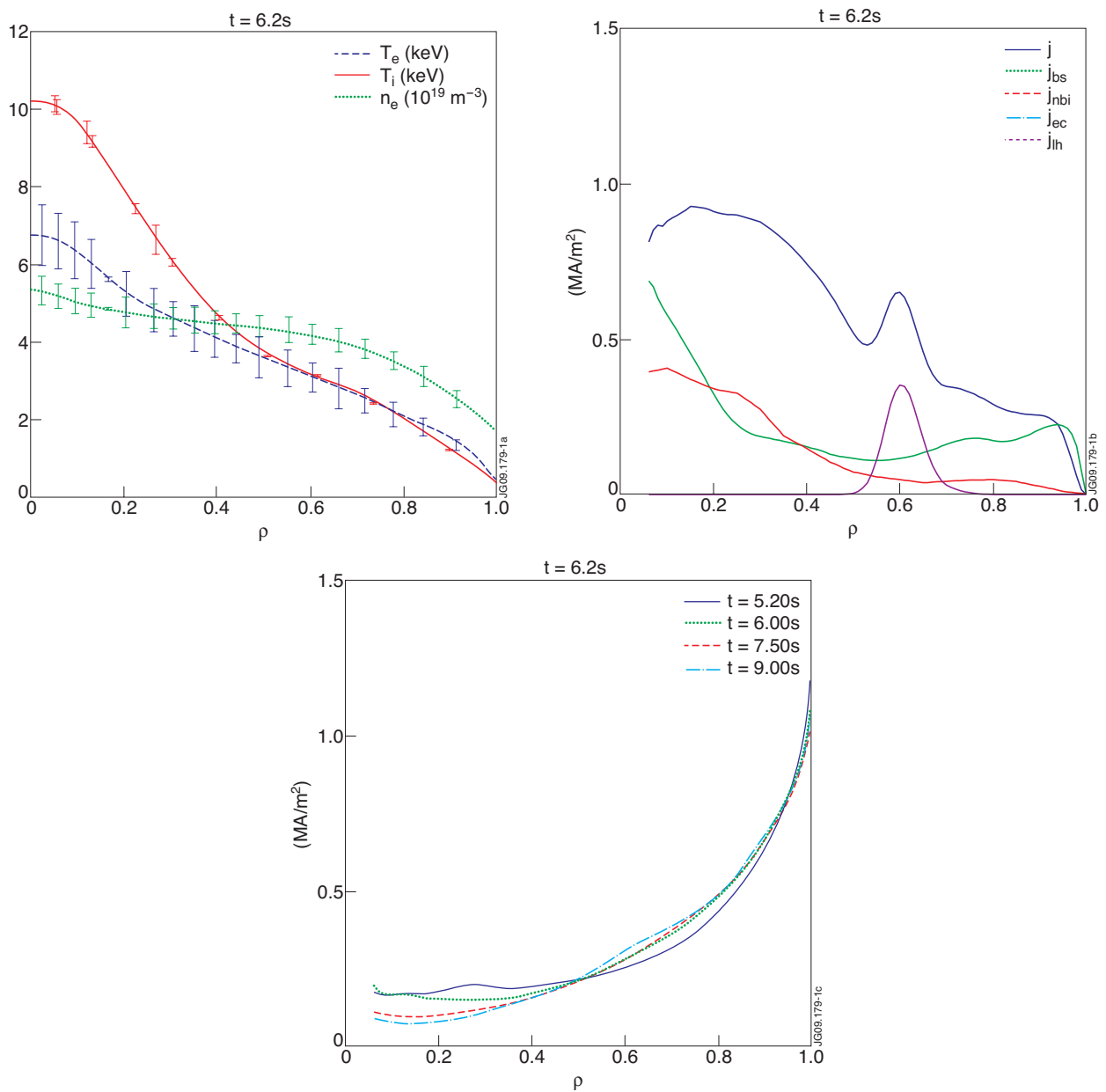


Figure 1: Electron, ion temperature and density profiles at $t = 6.2s$ for Pulse No: 77895 (a). Total current (j), bootstrap current (j_{bs}), NBI (j_{nbi}) and lower hybrid (j_{lh}) current drive density profiles at $t = 6.2s$ for Pulse No: 77895 (b). Evolution of the q profile calculated with CRONOS for Pulse No: 77895 (c).

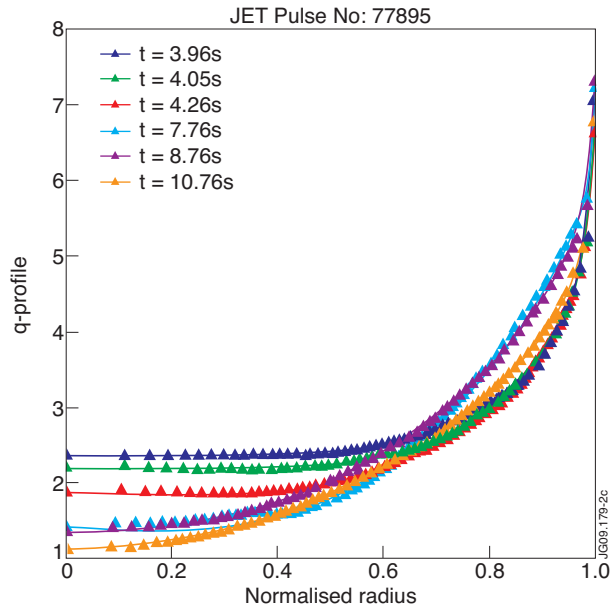


Figure 2: Experimental q profiles calculated with EFIT constrained with MSE data.

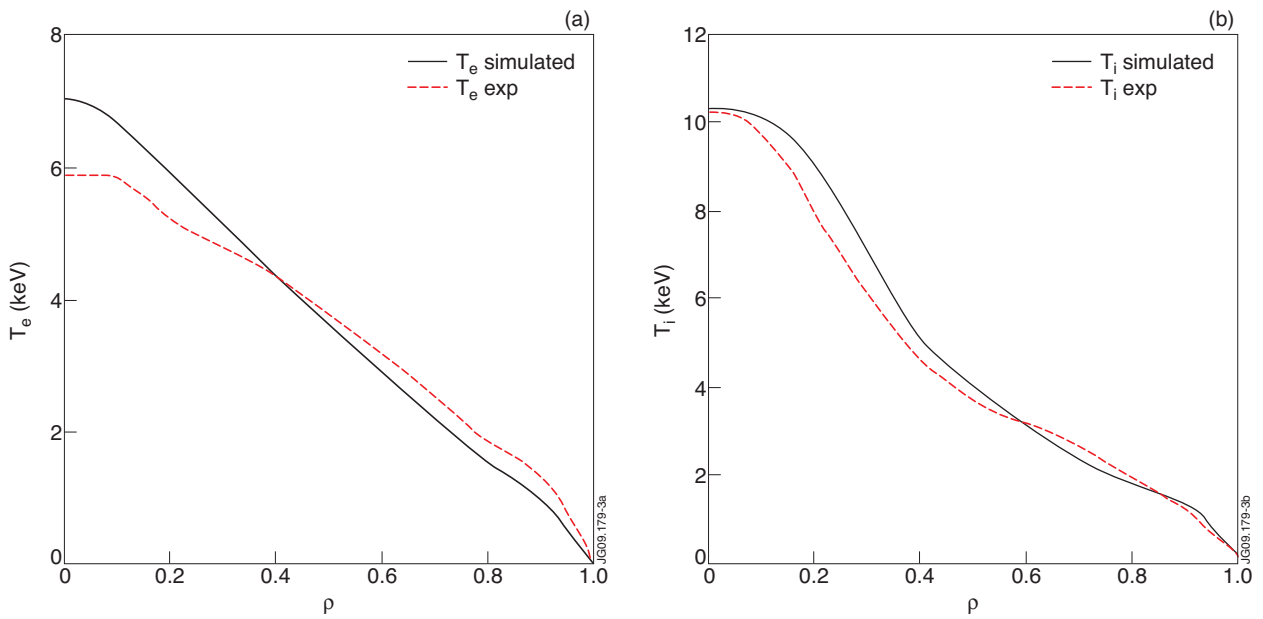


Figure 3: Comparison between experimental electron temperature profile for Pulse No: 77895 and simulated one (a) Comparison between experimental ion temperature profile for Pulse No: 77895 and simulated one (b).

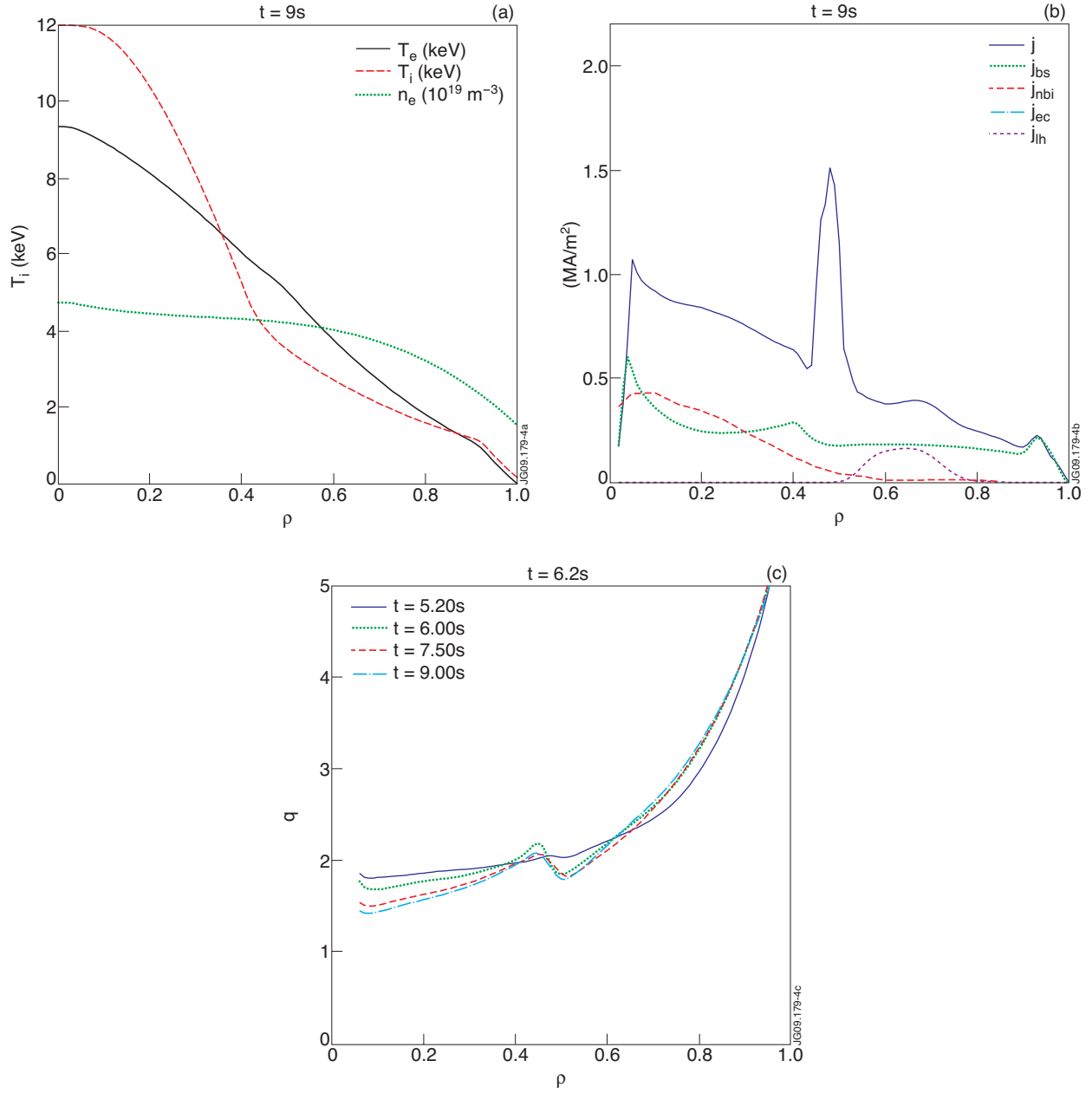


Figure 4: Electron, ion temperature and density profiles at $t=9s$ (a). Total current (j), bootstrap current (j_{bs}), NBI (j_{nbi}), lower hybrid (j_{lh}) and electron cyclotron (j_{ec}) current drive density profiles at $t=9s$ (b). Evolution of the q profile calculated with CRONOS(c).

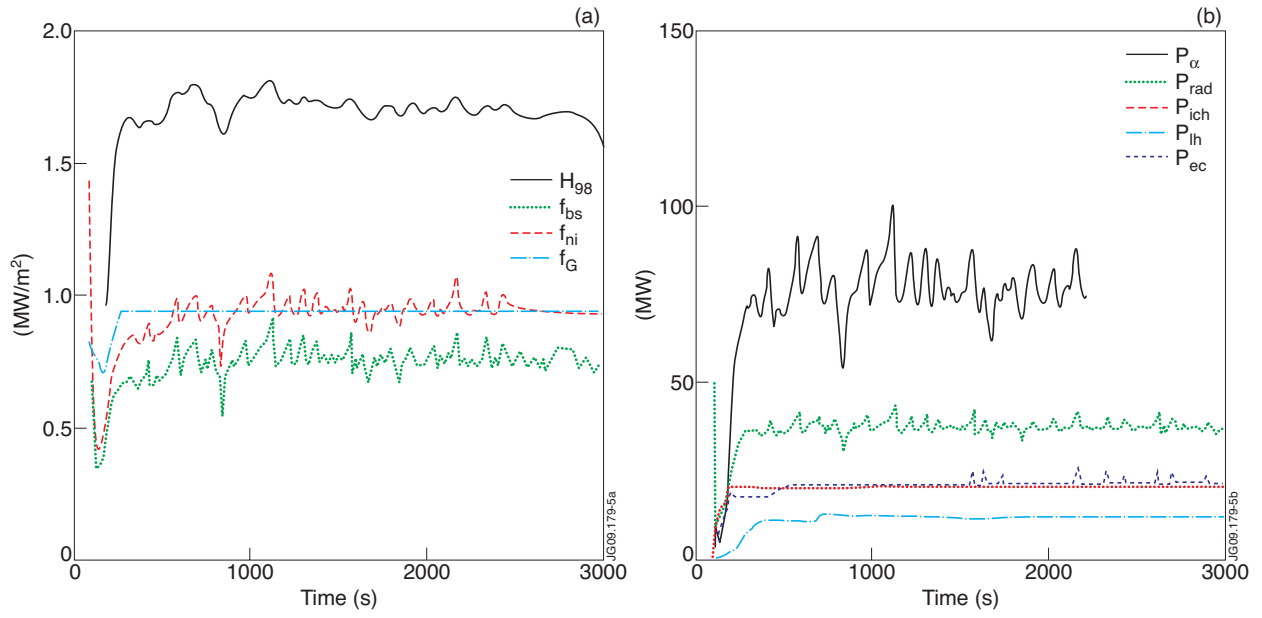


Figure 5: Time evolution of H_{98} , f_{bs} , f_{ni} and f_G . (a) Time evolution of alpha (P_{α}), radiated (P_{rad}), ICRH (P_{ich}), LH (P_{lh}) and EC (P_{ec}) power (b).

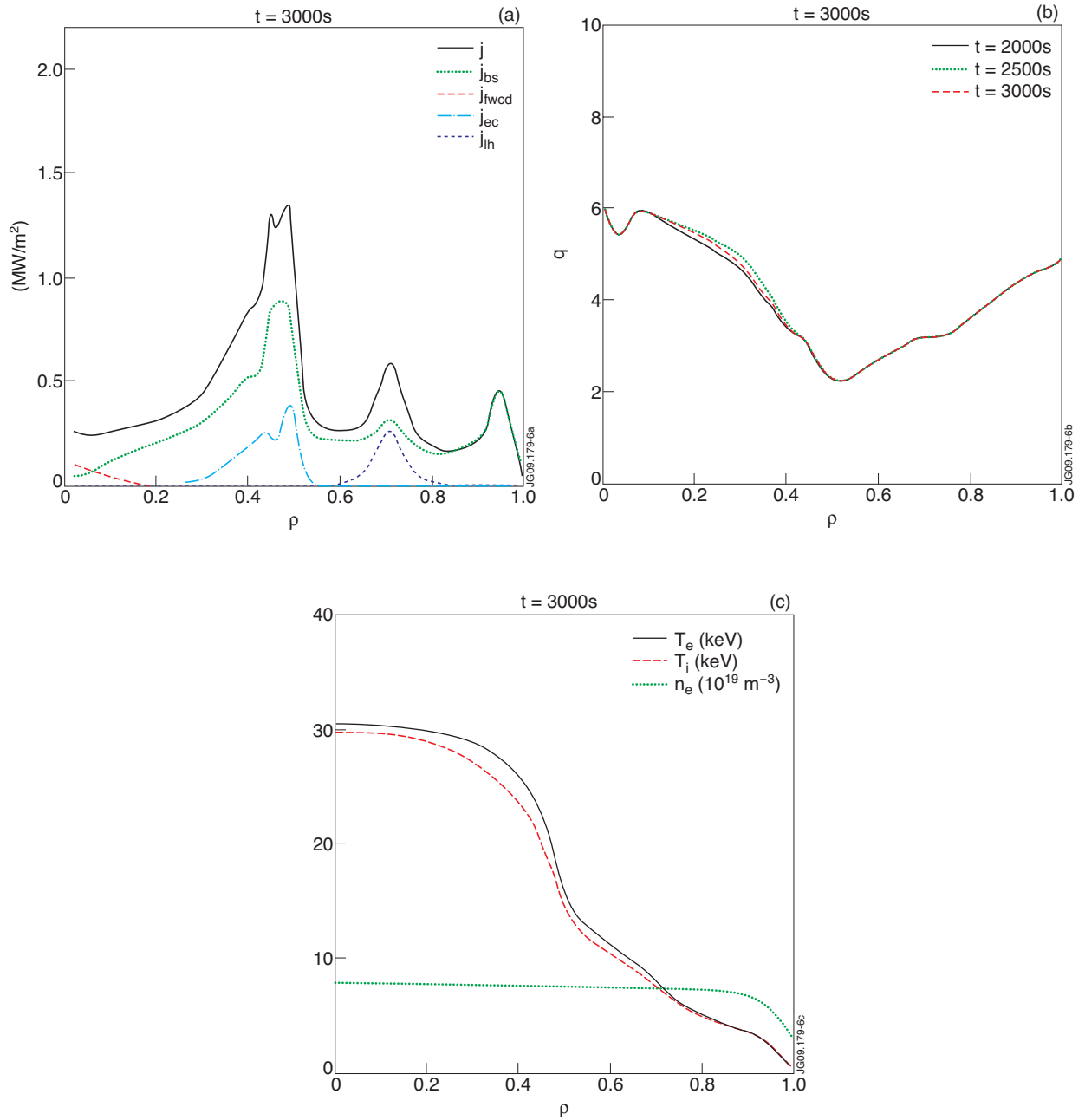


Figure 6: Total current (j), bootstrap current (j_{bs}), fast wave (j_{fwcd}), electron cyclotron (j_{ec}) and lower hybrid (j_{lh}) current drive density profiles at $t=3000s$ (a). Evolution of the q profile (b). Electron, ion temperature and density profiles at $t=3000s$. (c).

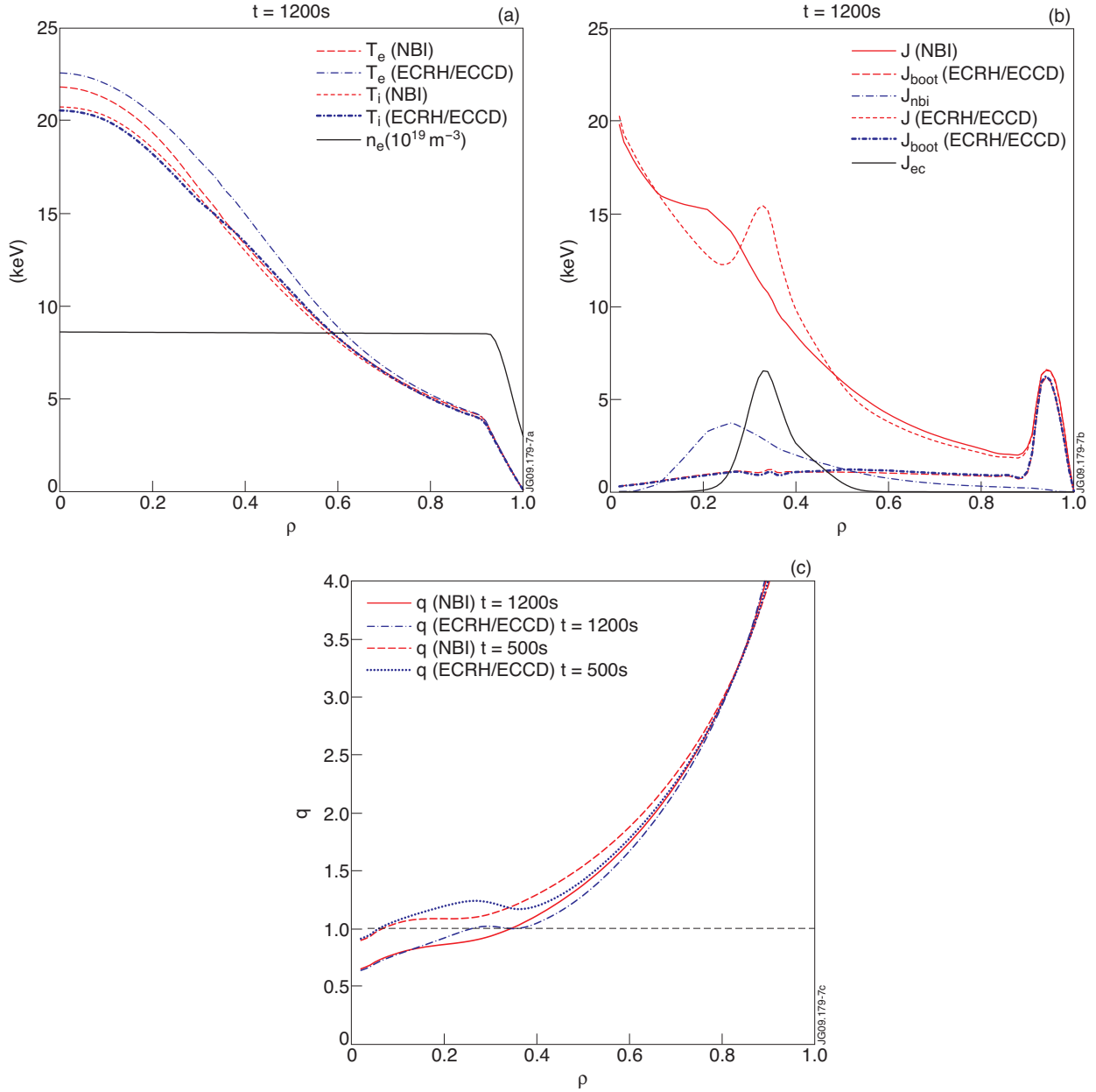


Figure 7: Electron, ion temperature and density profiles at $t=1200s$ (a). Total current (j), bootstrap current (j_{bs}), NBI (j_{nbi}), lower hybrid (j_{lh}) and electron cyclotron (j_{ec}) current drive density profiles at $t=1200s$ (b). Evolution of the q profile (c).